
ROUTE CHOICE-BASED SOCIO-TECHNICAL MACROSCOPIC TRAFFIC MODEL

Tanushree Roy

Department of Mechanical Engineering
The Pennsylvania State University
University Park, PA 16802, USA.
tbr5281@psu.edu

Satadru Dey

Department of Mechanical Engineering
The Pennsylvania State University
University Park, PA 16802, USA.
skd5685@psu.edu

January 4, 2021

ABSTRACT

Human route choice is undeniably one of the key contributing factors towards traffic dynamics. However, most existing macroscopic traffic models are typically concerned with driving behavior and do not incorporate human route choice behavior models in their formulation. In this paper, we propose a socio-technical macroscopic traffic model that characterizes the traffic states using human route choice attributes. Essentially, such model provides a framework for capturing the Cyber-Physical-Social coupling in smart transportation systems. To derive this model, we first use Cumulative Prospect Theory (CPT) to model the human passengers' route choice under bounded rationality. These choices are assumed to be influenced by traffic alerts and other incomplete traffic information. Next, we assume that the vehicles are operating under a non-cooperative cruise control scenario. Accordingly, human route choice segregates the traffic into multiple classes where each class corresponds to a specific route between an origin-destination pair. Thereafter, we derive a Mean Field Game (MFG) limit of this non-cooperative game to obtain a macroscopic model which embeds the human route choice attribute. Finally, we analyze the mathematical characteristics of the proposed model and present simulation studies to illustrate the model behavior.

1 Introduction

Modern Intelligent Transportation Systems (ITSs) exhibit strong interactions between Information & Communication Technology (ICT), physical traffic flow, and human social behavior. Such interaction is even stronger in smart mobility solutions such as Connected Adaptive Cruise Control (CACC) systems. This motivates the need for modeling traffic dynamics in ITSs as socio-technical systems which capture the Cyber-Physical-Social coupling [38]. Essentially, human cognitive and social behavior is incorporated with the physical vehicular dynamics and cybernetic strategies of the smart mobility solutions in this type of socio-technical models. Such modeling strategies have the potential to provide a quantifiable connection between smart mobility dynamics and human behavioral dynamics. Along this line, this paper presents a socio-technical modeling framework for traffic systems that characterizes the macroscopic traffic dynamics in terms of the decision behavior of the human-in-the-vehicle, under a CACC driving scenario.

In literature there exist different frameworks for modeling human behavioral aspects, Cumulative Prospect Theory (CPT) being one of them [32]. Within this framework, the behavior of humans as decision makers under uncertainty is of bounded rationality. Essentially, CPT models this decision behavior using subjective utility of outcome and subjective perception of probability. CPT was originally proposed in the context of economics, and later applied to human-in-the-loop technical systems. For example, CPT is employed in consumer-behavior based electricity pricing [20], cloud-storage defense strategy [42], and evaluation of renewable power sources [40]. In transportation related applications, CPT has been explored in passenger behavior modeling based on waiting time [1], driver behavior in context changing to High-Occupancy-Vehicle lanes [4], interaction framework between traffic information provider and user modeled as a Stackelberg game [17], developing adaptive pricing strategies for Shared Mobility on Demand Services [16]. Besides, CPT has been explored in the context of modeling driver route choice behavior

where the traveller has incomplete traffic information [43], friends' travel information [45], and traffic information through variable message sign indicators [12, 13]. In [2], Logit Kernel to model human route choice as a function of travel time information. Nevertheless, these aforementioned works do not to explore the impact of such human route choices on macroscopic traffic behavior. This is especially relevant now because of the increasing distribution of traffic information through platforms such Google Maps and INRIX.

Existing traffic modeling strategies can be generally categorized into two classes: (i) vehicle-based or microscopic, and (ii) traffic flow-based or macroscopic. In literature, microscopic modeling of Adaptive Cruise Control (ACC) enabled cars in the cooperative setting has been explored in [5, 23, 35, 36, 41] while ACC under non-cooperative setting has been addressed in [31, 34, 44]. The inherent disadvantage of such microscopic models is the computational burden for increased number of vehicles. Hence, efforts have been made towards macroscopic modeling of ACC enabled traffic flow in cooperative [6, 24] and non-cooperative [18, 19, 25] settings. Additionally, in [11, 22, 30], interactions between individual autonomous vehicle and human-driven vehicle or pedestrian have been investigated. In [19], a macroscopic model traffic flow model for autonomous vehicles has been derived using Mean Field Games (MFG) by connecting microscopic vehicular dynamics to macroscopic traffic flow. Additionally, the same authors extended their work in [18] to capture traffic dynamics in a mixed traffic scenario containing autonomous vehicles and human-driven vehicles. However, in [18, 19], the human-driven vehicles lack human behavioral models and autonomous vehicles were modelled as rational agents. Hence, these works do not address the impact of route choices made by the human passengers on macroscopic traffic flow. In our present paper, we utilize MFG setting (similar to the one discussed in [19]) to connect microscopic dynamics to macroscopic models, and propose a modeling framework to capture the human behavioral aspects in macroscopic traffic dynamics. Such incorporation of human behavioral aspects enables understanding of traffic dynamics in realistic settings with cyber-physical-social interactions. This is essential since even with fully autonomous vehicles, some features such as choice of routes will often lie with the human passengers [39]. Evidently, these choices would be influenced by human behavior and the incomplete traffic information available to them.

To address the aforementioned gap, the main contribution of the paper is a socio-technical macroscopic traffic flow model with human route choice attributes. Specifically, we formulate a multi-class model for non-cooperative CACC enabled vehicle traffic flow, which is parameterized by outputs from human route choice behavior model. We have modelled the human decision making behavior using CPT where the utility of choosing a specific route depends on the incoming traffic information and driving convenience knowledge about each route, e.g. general road conditions and presence of tolls. Needless to say, this route choice behavior dictates the number vehicle along each route. Next, we have assumed that all vehicles are non-cooperatively optimizing their cost functional along the chosen route which in turn leads to a differential game setting. In order to transition from this microscopic setting to macroscopic traffic characteristics, we take Mean Field Game (MFG) limit of this differential game. Subsequently, we obtain a multi-class model for the macroscopic traffic flow that provides the continuum equation as well as the dynamics of the driving cost. Here, this driving cost embeds the human route choice behavior as an attribute of the traffic flow. We also analyze the following mathematical properties of the socio-technical traffic model: (i) Fundamental Diagram, (ii) hyperbolicity, and (iii) Lyapunov-based linear stability.

This paper is organized as follows. Section II discusses the Problem statement of the paper, Section III develops the modeling framework, Section IV proposed the Socio-technical model for traffic, Section V discusses a case study, Section VI shows the simulation results of our work followed by conclusion in Section VII.

2 Problem Statement

We consider a macroscopic traffic flow of CACC enabled connected and autonomous vehicles between single Origin-Destination (OD) pair A and C as shown in Figure 1. Without loss of generality, we consider two routes between this OD pair that fork at junction C, as shown in Figure 1. At junction C, each vehicle has to choose either Route 1 or 2. Such choice is made by the human passenger in the vehicle based on the accessible route information. Essentially, the traffic flow starting at Origin A divides into two streams at junction C, where one stream takes Route 1 and the other stream takes Route 2. Next, we make the following assumptions regarding our problem setting.

Assumption 1. *Each vehicle is occupied by a passenger who has control over vehicle route selection.*

Assumption 2. *Routes 1 and 2 have different characteristics in terms of estimated travel time, maximum density, and road condition. As expected, these factors influence the decision of the human passenger in the vehicle to opt for a specific route. Additionally, we assume that the condition of these routes are dynamically changing with time. For example, such changes can occur due to accidents, unpredictable road conditions from construction work or pedestrian traffic.*

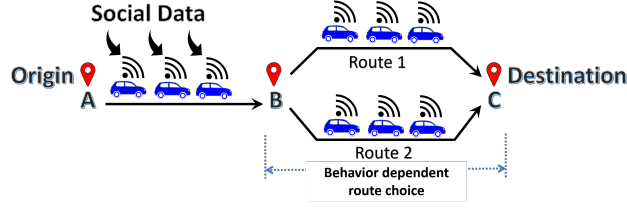


Figure 1: Socio-Technical traffic dynamics.

Assumption 3. *The human passenger in the vehicle has partial information about changing characteristics of each route through various traffic reporting platforms such as Google Maps, MapQuest, INRIX, twitter feeds, and cell phone texts. Such an assumption is reasonable in light of the extensive dissemination of social data in today's world [7].*

Assumption 4. *Due to the presence of partial or incomplete information, the human passenger is assumed to be a bounded rational agent where their preferences are motivated to maximize the utility of a choice.*

Assumption 5. *All the vehicles are identical in terms of physical structure and CACC driving capabilities. While behavior of vehicles choosing a specific route are homogeneous within the group, groups of vehicle corresponding to each route differ from one another in terms of the driving costs. In other other words, depending on the choice of route the vehicles are grouped into classes that are dependent on the costs to drive on that particular route.*

Assumption 6. *All vehicles receive certain traffic updates through traffic reporting platforms at the same time.*

Based on the aforementioned setting, our goal is to model the macroscopic traffic dynamics in the whole segment A-B-C, characterized by the behavioral dynamics of the human passengers. To develop this modeling strategy, we execute the following steps. A schematic of the model development framework is shown in Fig. 2.

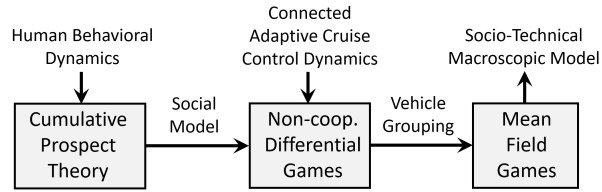


Figure 2: Socio-Technical macroscopic traffic modeling framework.

Step 1: First, we model the human choice dynamics using Cumulative Prospect Theory (CPT) which takes into account human behavioral traits such as loss aversion, perception of loss or gain of an outcome dependent on some reference and under-weighting common events while over-weighting unlikely events. Depending on the probability of each human passenger to choose a particular route, the number of vehicles that will proceed towards Route $j \in \{1, 2\}$ is decided.

Step 2: Next, utilizing these two groups of vehicles (corresponding to two routes), a non-cooperative differential game is set up such that (i) vehicles in each group try to obtain a minimum driving cost, and (ii) vehicles in one group maintain safety from other group of vehicles.

Step 3: Subsequently, we take an arbitrarily large limit for each group of vehicles to derive a Mean Field Games (MFG). This generates a multi-class macroscopic traffic flow model of CACC-enabled vehicles. This multi-class macroscopic model is a socio-technical traffic model since human route choice attribute parameterizes its Fundamental Diagram.

In the next section, we discuss these steps in detail.

3 Model Development Framework

In this section, we detail the model development framework. We start with CPT based modeling of human choice behavior followed by differential and mean field games based macroscopic models.

3.1 Modeling Route Choice Based on Traffic Alerts

The route selection decision of human passenger under the influence of traffic alerts can be modeled using Cumulative Prospect theory (CPT). The behavior of humans as decision makers under uncertainty is of bounded rationality [15]. CPT models this decision behavior using subjective utility of outcome and subjective perception of probability [32]. The prospect value of choosing a route is uncertain due to various reasons such as congestion, unpredictable road conditions among many others. As described before, we assume two possible prospects: either someone chooses Route 1 or Route 2. We intend to utilize CPT to obtain the probability of people who would act favourably on receiving a traffic alerts suggesting a change from Route 1 to 2. In other words, we compute the fraction of people who would change their route from Route 1 to 2 upon receiving a route change recommendation. This fraction depends on the subjective perception of the prospect value of a choice and can be modeled using CPT in the following way.

A prospect j is denoted by a sequence of pairs consisting of utility or value (of loss or gain) and probability (of loss or gain), for N_j possible outcomes i.e. $(z_1^j, p_1^j, \dots, z_{N_j}^j, p_{N_j}^j)$ where z_i^j are the utilities (modeled as discrete random variables) and p_i^j are the corresponding probabilities with $i \in \{1, \dots, N_j\}$. Consequently, the objective value of a prospect is given by [32]

$$\mathbb{U}_o^j = \sum_{i=1}^{N_j} z_i^j p_i^j. \quad (1)$$

In our problem set-up, there are two prospects that the human decision maker is choosing from: Route 1 and Route 2. Hence in our case $j \in \{1, 2\}$.

However, human decisions are most often subjective and far from rational. That is, the utility and probability of each outcome is perceived differently. CPT formulates this modification of utility and probability under the following axioms of human decision phenomenon [32].

Subjective Utility: The perceived gain or loss value of an outcome is affected by the following factors:

- *Framing Effect:* Subjective loss or gain from a prospect is perceived with respect to a reference value.
- *Loss Aversion:* Humans are more affected by a loss than an equal amount of gain. This causes a difference in how loss or gain of a prospect is perceived subjectively and leads to an attitude of risk aversion in face of loss outcome.
- *Diminishing Value Sensitivity:* Individuals are less affected by *changes* in loss (gain) when the value of the prospect is already in high losses (high gains).

Probability Distortion: The perception of probability of an outcome is affected by the following factors:

- *Over/Underweighting:* Human decision behavior is highly influenced by unlikely events while ignoring highly probable events i.e. low probability events are over-weighted compared to highly probability events.
- *Increased Probability Sensitivity:* Near the end points of probability $p = 0$ and $p = 1$, changes in probability is perceived more than for mid-range probability.
- *Relative sensitivity:* Different attitudes associated towards probabilities for gain and losses are observed and are listed as follows: (i) Risk aversion over gains of high probability, (ii) Risk aversion over losses of small probability, (iii) Risk seeking over gains of low probability and (iv) Risk seeking over losses of high probability.

Motivated by these axioms, the subjective utility of an outcome can be modeled by the value (or utility) function $z \rightarrow U(z)$ given by

$$U(z) = \begin{cases} (z - R)^{\beta^+}, & \text{if } z > R, \\ -\lambda(R - z)^{\beta^-}, & \text{otherwise,} \end{cases} \quad (2)$$

where R is the reference for loss or gain, $\lambda > 1$ denotes loss aversion, and $\beta^+ > 0$ and $\beta^- < 1$ denote the diminishing sensitivities to loss or gain.

Let the utilities be arranged in an ascending order from maximum loss to maximum gain, i.e. $z_1^j \leq z_2^j \leq \dots \leq z_g^j \leq 0 \leq z_{g+1}^j \leq \dots \leq z_{N_j}^j$ for a given prospect j . Here positive utilities imply gains and non-positive utilities imply losses. Let the probability corresponding to these utilities are given by $p_1^j, p_2^j, \dots, p_g^j, p_{g+1}^j, \dots, p_{N_j}^j$. Then the

probability distortion experienced by a limited rational human decision maker is given by the probability weighting function $w(p)$ defined as

$$w(p) = e^{-(-\ln p)^\gamma}. \quad (3)$$

The function $w(\cdot)$ is known as the Prelec's function [28]. For $0 < \gamma < 1$, it produces the characteristic inverse-S shaped curve showing the desired probability distortion characteristics. In order to capture the four risk seeking or avoiding characteristics (mentioned under *Relative Sensitivity* above), CPT defines $\pi_1^{j-}, \dots, \pi_g^{j-}$ as the transformation of the probability for loss, and $\pi_{g+1}^{j+}, \dots, \pi_{N_j}^{j+}$ as the transformation of the probability for gain, which are given by [10]

$$\pi_1^{j-} = w(p_1^j), \quad (4)$$

$$\pi_i^{j-} = w\left(\sum_{m=1}^i p_m^j\right) - w\left(\sum_{m=1}^{i-1} p_m^j\right), \quad (5)$$

where $2 \leq i \leq g$, and

$$\pi_{N_j}^{j+} = w(p_{N_j}^j), \quad (6)$$

$$\pi_i^{j+} = w\left(\sum_{m=i}^{N_j} p_m^j\right) - w\left(\sum_{m=i+1}^{N_j} p_m^j\right), \quad (7)$$

where $g+1 \leq i \leq N_j-1$. The transformations $\pi_1^{j-}, \dots, \pi_g^{j-}, \pi_{g+1}^{j+}, \dots, \pi_{N_j}^{j+}$ essentially are the decision weights for each outcome z_i^j . Subsequently, the overall CPT (subjective) value of a prospect j is given by

$$\mathbb{U}_j = \sum_{i=1}^g \pi_i^{j-} U(z_i^j) + \sum_{i=g+1}^{N_j} \pi_i^{j+} U(z_i^j). \quad (8)$$

Next, consider the case where we have utility \mathbb{Z} as a continuous random variable as opposed to discrete utility variables $z_i^j, i \in \{1, \dots, N_j\}$. The probability and complimentary distribution functions of this continuous random utility \mathbb{Z} are related to the discrete probability distribution by the following:

$$F_{\mathbb{Z}}(z_i^j) = P(\mathbb{Z} \leq z_i^j) = \sum_{z_g^j \leq z_i^j} p(z_g^j) = \sum_{g=1}^i p_g^j, \quad (9)$$

$$F_{\mathbb{Z}}(z_{i-1}^j) = P(\mathbb{Z} > z_{i-1}^j) = \sum_{z_g^j > z_{i-1}^j} p(z_g^j) = \sum_{g=i}^{N_j} p_g^j. \quad (10)$$

Accordingly, the overall CPT (subjective) value of a prospect j (8) can be re-written as

$$\mathbb{U}_j = \int_{-\infty}^R U(z) \frac{d}{dz} \{\pi(F_{\mathbb{Z}}(z))\} dx + \int_R^{\infty} U(z) \frac{d}{dz} \{-\pi(1 - F_{\mathbb{Z}}(z))\} dx.$$

where R is the reference for loss or gain, defined in (2). That is, R is the certain level of utility that the human passenger perceives as needed to reach to the destination. For example, before starting the journey the human passenger allots certain amount of time to reach the destination and any deviation from that will be perceived as a *gain* or *loss* depending on whether they arrive earlier or later than their allotted time, respectively.

Next, we define the utilities of possible outcomes and their probabilities. For any prospect or choice of route, the outcome is stochastic as it depends on various factors [2]. Among these, we consider the effect of incoming traffic alerts from various traffic reporting platforms on the human passenger. Apart from the traffic alerts, we may also consider other stochastic factors that affect a human's decision to choose a route such as stochastic travel time, ease of navigation on a road, additional tariff etc. Here, we assume the utility of choosing a route to be a continuous random variable that depends on: (i) incoming traffic alerts, (ii) priority/veracity of these data, (iii) estimated travel time, and (iv) other fixed driving factors. Consequently, we represent the utility random variable as follows:

$$\mathbb{Z} = a_1 S_1 + \dots + a_M S_M + k_1 T + k_2, \quad (11)$$

where $S_1, \dots, S_M \in \{0, 1\}$ are incoming traffic alerts that follow Poisson Distribution; the weights a_1, \dots, a_M represents the decision maker's trust in or potential to act to each of these alerts; T is stochastic travel time with k_1 as a weight; and k_2 captures the fixed driving convenience factors such as absence of toll, not leading to congested neighborhood detours, familiarity with the route, general road condition knowledge among many other factors. These weights are chosen to make \mathbb{Z} dimension-less and to normalize each terms. Continuous travel time random variable T is assumed to have a truncated normal distribution.

Thereafter, a logit model is used to predict the probability of an outcome. This enables us to capture the probabilistic nature of human decision making [26]. We define the utility random variable for the human passenger in k -th vehicle to be \mathbb{U}^k and the corresponding CPT (subjective) utility value to be \mathbb{U}_j^k . Hence, the probability of human passenger in k -th vehicle to choose Route j is given by the logit model as follows [26]:

$$p_j^k = \frac{e^{\phi \mathbb{U}_j^k}}{e^{\phi \mathbb{U}_1^k} + e^{\phi \mathbb{U}_2^k}}, \forall j \in \{1, 2\}, \quad (12)$$

where parameter $\phi > 0$ is the sensitivity parameter which determines how the decision making is sensitive to individual utility. For example, with $\phi = 0$, the choice is random and is unaffected by utility of either choice. With increasing ϕ , the probability is affected increasingly more by the difference in utility of the choices. This can be easily seen by the alternate form of this logit model, for say Route 1: $p_1^k = 1/(1 + e^{\phi(\mathbb{U}_2^k - \mathbb{U}_1^k)})$ where even small difference $(\mathbb{U}_2^k - \mathbb{U}_1^k)$ will significantly affect p_1^k when ϕ is large.

Now, we compute \mathcal{M}_j , the number of human passengers who choose Route j by aggregating the maximum probability of choosing that route for individual vehicles:

$$\mathcal{M}_j := \left| \left\{ m : \operatorname{argmax}_{m \in \{1, 2\}} p_m^k = j, \forall k \in \{1, \dots, \mathcal{M}\} \right\} \right|. \quad (13)$$

We note here that the probability p_j^k is dependent on the traffic alerts S_1, \dots, S_M , weighting parameters a_1, \dots, a_M , travel time T , scaling parameter k_1 , driving convenience factors k_2 as well as parameters of human choice behavior given by $R, \beta^+, \beta^-, \lambda, \gamma$ and ϕ . Defining a vector containing *social* signals and parameters as

$$\sigma = [S_1, \dots, S_M, a_1, \dots, a_M, T, k_1, k_2, R, \beta^+, \beta^-, \lambda, \gamma, \phi],$$

we can write \mathcal{M}_j to be a function of σ , that is $\mathcal{M}_j(\sigma)$.

Remark 1. *The parameters of the human behavior model can be estimated by collecting data through behavioral experiments or surveys [37, 45]. In order to capture the parameters accurately, the participant sample should also be varied in terms of age, gender, race, financial standing and technological proficiency. These data collection strategies would record human route choice outcome under various scenarios of traffic alerts and other traffic information.*

3.2 CACC as a Differential Game

In this problem, we assume that the vehicles in the traffic is Connected Adaptive Cruise Control (CACC) enabled. In this setting, the velocity of the vehicles are calculated with the information of other vehicles by solving an optimization problem [34]. Denoting the position and velocity of k -th vehicle opting Route j by x_j^k and v_j^k , respectively, the vehicle dynamics equation is given by

$$\dot{x}_j^k(\zeta) = v_j^k(\zeta), \quad x_j^k(t) = x_j^k, \quad (14)$$

for $j \in \{1, 2\}$ and $k \in \{1, \dots, \mathcal{M}_j(\sigma)\}$ where $\mathcal{M}_j(\sigma)$ represents the number of vehicle choosing Route j . Additionally, for the k -th vehicle the driving overhead for choosing Route j can be represented by the following functional:

$$\mathcal{H}_j^k(v_j^k, \tilde{v}_j^k) = \int_{t_0}^t F^{\mathcal{M}_j}(v_j^k(\zeta), \tilde{x}_j^k(\zeta), \mathbf{x}_{\sim j}^k(\zeta), \mathbf{x}_{\sim j}(\zeta)) d\zeta + R(x_j^k(t_0)),$$

where $\mathbf{x}_{\sim j}^k(t) = \{x_j^1(t), \dots, x_j^{k-1}(t), x_j^{k+1}(t), \dots, x_j^{\mathcal{M}_j}(t)\}$ represents the positions of all vehicles except k -th vehicle that are opting for Route j , $\mathbf{x}_{\sim j}$ represents positions of all vehicles opting for routes other than j , v_j^k is the velocity of k -th vehicle opting for Route j and $\tilde{v}_j^k(t)$ is velocity of all vehicles other the k -th vehicle opting for Route j . Here, $F^{\mathcal{M}_j}$ is a cost functional whose form is identical for all vehicles along Route j and $R(x_j^k(t_0))$ is the *starting penalty* along Route j which depends on the initial position of the k -th vehicle (Route j) at time $t = t_0$ (refer to (14)). We assume that the cost functional $F^{\mathcal{M}_j}$ is strictly convex with respect to the variable $v_j^k(t)$ for the existence of solution to the Hamilton-Jacobi-Bellman (HJB) equation [21].

In this setting, we assume that all the vehicles have same free-flow velocity v_{max} . Hence, the optimal velocity $u_j^k \in (0, v_{max}]$ for the k -th vehicle minimizes the driving cost among all other vehicles such that $\mathcal{H}_j^k(u_j^k, v_j^{\sim k}) \leq \mathcal{H}_j^k(v_j^k, v_j^{\sim k})$. Consequently, every vehicle solves this optimal solution simultaneously to form a non-cooperative multi-vehicle differential games.

3.3 Limiting Mean Field Game

Generally speaking, solving the aforementioned non-cooperative multi-vehicle game is exceedingly hard with increased number of vehicles. This motivates the introduction of Mean Field Games (MFG) which is a non-cooperative game with arbitrarily large number of players [3]. Unlike finite differential games where each player interacts with every other player, in MFG individual interactions are *smoothed out* in the sense that coupling between players is only through the interaction with the average behavior or *mean field*. In MFG limit of our differential games among vehicles, a global traffic behavior emerges from the collective interactions of vehicles, as derived in [19].

Following [19], we use the concept of traffic density in order to smoothen the position information of the vehicles. This density function can be constructed using Kernel Density Estimation (KDE). Here, we use the Parzen-Rosenblatt window method [27, 29] that *smooths out* the position information over window length a to produce local density information. First, the position information is captured using a Dirac comb function $C(x) = \frac{1}{N} \sum_{k=1}^N \delta(x - x_k)$. Subsequently, $C(x)$ is smoothed to the density function

$$\rho^{\mathcal{M}} = \int_{\mathbb{R}} \Phi_a(x - y) C(y) dy = \frac{1}{\mathcal{M}} \sum_{k=1}^{\mathcal{M}} \Phi_a(x - x_j), \quad (15)$$

where the Gaussian Smoothing kernel $\Phi_a(x)$ is given by

$$\Phi_a(x) = \frac{1}{\sqrt{2\pi}a} \exp\left(-\frac{x^2}{2a^2}\right). \quad (16)$$

Accordingly, the smoothed total density function in our problem is derived as

$$\begin{aligned} \rho^{\mathcal{M}}(x_1, x_2, t) &= \frac{1}{\mathcal{M}_1 + \mathcal{M}_2} \left[\sum_{k=1}^{\mathcal{M}_1} \Phi_a(x_1 - x_1^k(t)) + \sum_{k=1}^{\mathcal{M}_2} \Phi_a(x_2 - x_2^k(t)) \right] \\ &= \frac{\mathcal{M}_1}{\mathcal{M}_1 + \mathcal{M}_2} \rho^{\mathcal{M}_1}(x_1, t) + \frac{\mathcal{M}_2}{\mathcal{M}_1 + \mathcal{M}_2} \rho^{\mathcal{M}_2}(x_2, t), \end{aligned} \quad (17)$$

where $\rho^{\mathcal{M}_j}(x_j, t) = \frac{1}{\mathcal{M}_j} \sum_{k=1}^{\mathcal{M}_j} \Phi_a(x_j - x_1^k)$ and $\mathcal{M} = \mathcal{M}_1 + \mathcal{M}_2$ is the total number of vehicles. The global cost functional can now be expressed in terms of smooth density information instead of discrete positions of individual vehicles as follows [3]:

$$F^{\mathcal{M}_j}(v_j^k(t), x_j^k(t), \mathbf{x}_j^{\sim k}(t), \mathbf{x}_{\sim j}(t)) := F(v_j(t), \rho^{\mathcal{M}_j}(x_j(t), t), \rho^{\mathcal{M}_{\sim j}}(x_{\sim j}(t), t), \alpha_j), \quad (18)$$

where $\alpha_j = \frac{\mathcal{M}_j}{\mathcal{M}_1 + \mathcal{M}_2}$. Here $\rho^{\mathcal{M}_{\sim j}}$ represents the density of the vehicles not choosing Route j . Notably, we observe here that the driving cost functional is affected by parameter α_j which in turn is dependent on the output of human route choice model as shown in (13).

Next, we obtain the MFG limit by making the number vehicles \mathcal{M}_1 and \mathcal{M}_2 to be arbitrarily large such that $\frac{\mathcal{M}_1}{\mathcal{M}_2} \rightarrow \kappa$ where $0 < \kappa < \infty$. This implies that limit to infinity of both kinds of vehicles must be of the same order. We also make the smoothing parameter a in (16) arbitrarily small such that $a/\mathcal{M}_j \rightarrow 0, \forall j$. This implies that on a finite road with increasing number of vehicles and shrinking *window* of density contribution from each vehicle, the local density will eventually describe the global density.

As $\mathcal{M}_j \rightarrow \infty$, $\rho^{\mathcal{M}_j}(x_j, t) \rightarrow \rho_j(x_j, t)$ which describes the density of the traffic when *only* vehicles in Route j was travelling on the road of interest. On the other hand, as both $\mathcal{M}_1, \mathcal{M}_2 \rightarrow \infty$ the *effective* density of the traffic due to all classes of vehicles is given by $\rho(x, t)$. Then (17) yields

$$\rho(x, t) = \alpha \rho_1(x, t) + (1 - \alpha) \rho_2(x, t), \quad (19)$$

where $\alpha = \frac{\kappa}{\kappa + 1}$ and $\rho_j(x, t) = \rho(x_j(t), t)$. From the assumptions of MFG limit, we can easily derive the bounds of α to be $0 < \alpha < 1$.

3.4 Socio-Technical Model

In this subsection, we derive the socio-technical macroscopic traffic model in two steps. Note that there are two classes of vehicles each corresponding to a particular route choice. First, we combine the theoretical tools discussed in Sections III.A, III.B, and III.C to develop the dynamics of class-specific traffic state which is dependent on human route choice. Second, we derive the continuity equation for traffic flow model for each class of vehicles.

Towards the first step, we consider the MFG setting where the position dynamics of the class of vehicles choosing Route j be represented by

$$\dot{x}_j(\zeta) = v_j(\zeta), \quad x_j(t_0) = x_0, \quad \zeta \in [t_0, t]. \quad (20)$$

Then, we define the optimal cost functional $\mathcal{H}_j(x, t)$ for the class of vehicles along Route j to reach position x at time t .

$$\mathcal{H}_j(x, t) = R(x_j(t_0)) + \min_{\substack{v_j(\tau) \\ t_0 \leq \tau \leq t}} \int_{t_0}^t F d\zeta, \quad (21)$$

where $F = F(v_j(\zeta), \rho_j(x, \zeta), \rho_{\sim j}(x, \zeta), \alpha)$, $v_j(\zeta)$ is generated from (20), and $x_j(t) = x$, $j \in \{1, 2\}$.

From the fundamentals of dynamic programming, we know that the optimal cost functional \mathcal{H}_j satisfies the HJB equation given as [21]:

$$\frac{\partial \mathcal{H}_j(x, t)}{\partial t} = \min_{v_j(t)} \left\{ F(v_j(t), \rho_j(x, t), \rho_{\sim j}(x, t), \alpha) - v_j(t) \frac{\partial \mathcal{H}_j}{\partial x} \right\}. \quad (22)$$

Thereafter, let us introduce the Legendre-Fenchel transform $F^* : (I^* \times \mathbb{R}^+ \times \mathbb{R}^+, \mathbb{R}^+) \rightarrow \mathbb{R}$ where $I^* = \{p \in \mathbb{R} : \min_{x \in \mathbb{R}} \{F(x, \rho_1, \rho_2, \alpha) - px\} < \infty\}$ and $F^*(p, \rho_1, \rho_2, \alpha) := \min_{x \in \mathbb{R}} \{F(x, \rho_1, \rho_2, \alpha) - xp\}$. This transform is well-defined for a convex function F . Furthermore, let us define $R(x_j(t_0)) := R_j(x_0)$. Also, define the optimal velocity solution for (22) to be $u_j(x, t)$. Then (22) can be equivalently written as a first order PDE

$$\frac{\partial \mathcal{H}_j(x, t)}{\partial t} = F^* \left(\frac{\partial \mathcal{H}_j(x, t)}{\partial x}, \rho_j(x, t), \rho_{\sim j}(x, t), \alpha \right), \quad (23)$$

and the optimal solution can be written as

$$u_j = F_w^*(w, \rho_j, \rho_{\sim j}, \alpha) \Big|_{w = \frac{\partial \mathcal{H}_j}{\partial x}}. \quad (24)$$

The initial condition for (23) is given by $\mathcal{H}_j(x, t_0) = R_j(x_0)$.

Next, towards the second step, we derive the continuum equation which provides the dynamical equation for the density of vehicles. This is derived from the set of conservation laws for a class of vehicles choosing a specific route and is given below [9]:

$$\frac{\partial \rho_j}{\partial t} + \frac{\partial(\rho_j u_j)}{\partial x} = 0, \quad j \in \{1, 2\}. \quad (25)$$

Now, we finally present the multi-class traffic model with a human choice attribute. The conservation of vehicles is obtained from (25) while the dynamics of the driving cost variable is obtained from (22) and (24). The final model equations reads

$$\frac{\partial \rho_j}{\partial t} + \frac{\partial(\rho_j u_j)}{\partial x} = 0, \quad (26)$$

$$\frac{\partial \mathcal{H}_j}{\partial t} + u_j \frac{\partial \mathcal{H}_j}{\partial x} = F(u_j, \rho, \rho_{\sim j}, \alpha), \quad (27)$$

$$u_j = \mathcal{I} \left(\frac{\partial \mathcal{H}_j}{\partial x}, \rho_j, \rho_{\sim j}, \alpha \right), \quad (28)$$

where $\mathcal{I} = F_w^*(w, \cdot)$ represents the velocity-density relation (Fundamental Diagram) which depends on the densities of the both class of vehicles. Note that \mathcal{I} is parameterized by the driving cost function $\frac{\partial \mathcal{H}_j}{\partial x}$ and human route choice parameter α . We also note from (21) that \mathcal{H}_j depends on human route choice parameter α . This in turn implies that the Fundamental Diagram is dependent on α implicitly through \mathcal{H}_j as well.

Defining a state vector

$$\eta(x, t) = [\rho_1(x, t), u_1(x, t), \rho_2(x, t), u_2(x, t)]^T, \quad (29)$$

we can write the boundary conditions for this system as

$$\eta(B^-, t) = G_B \eta(A^+, t), \quad \eta(C^-, t) = G_C \eta(B^+, t), \quad \forall t \in \mathbb{R}^+, \quad (30)$$

where G_B and G_C are 4×4 matrices. Moreover, the Rankine-Hugoniot Condition [14] provides the connection formula for conservation of fluxes before and after the juncture point B and is given by:

$$\alpha u_1(B^-, t) \rho_1(B^-, t) + (1 - \alpha) u_2(B^-, t) \rho_2(B^-, t) \quad (31)$$

$$= u_1(B^+, t) \rho_1(B^+, t) + u_2(B^+, t) \rho_2(B^+, t). \quad (32)$$

The initial condition for the model is

$$\eta(x, 0) = \eta_0. \quad (33)$$

Finally, the socio-technical model for human route choice is given by dynamical equations (26)-(28), boundary conditions (30), initial condition (33) and connection formula for the road juncture at B (31).

4 Mathematical Characteristics of the Socio-Technical Model

Depending on the driving objective of the CACC, we can choose various cost functionals $F(\cdot)$ in (27). To capture comparable impact of the terms in the cost functional, we assume that all variables are normalized.

$$F(u_j, \rho_1, \rho_2, \alpha) = \mathfrak{L}(x) F_j + (1 - \mathfrak{L}(x)) G_j, \quad (34)$$

$$F_1 = \frac{u_1^2}{2} - u_1 + \alpha u_1 \rho_1, \quad (35)$$

$$F_2 = \frac{u_2^2}{2} - u_2 + (1 - \alpha) u_2 \rho_2, \quad (36)$$

$$G_j = \frac{u_j^2}{2} - u_j + u_j \rho_j, \quad \forall j \in \{1, 2\}. \quad (37)$$

The cost functional F_j corresponds to the vehicles driving on main road (between A and B), and the cost functional G_j corresponds to the vehicles driving on the Route j (between C and D). The function $\mathfrak{L} = 1$ when the cars are in AB while $\mathfrak{L} = 0$ when they are on Route $j \in \{1, 2\}$. For functional F_j in (35)-(36), the first and second terms represent the kinetic energy and driving efficiency of the class of vehicles choosing Route j whereas the last term represents the driving safety of the vehicles of class j in response to the density of the vehicles of same class on the road. Similarly, for the functional G_j in (37), terms include kinetic energy, efficiency and the safety of vehicles on Route j .

Next, we analyse the model for $\mathfrak{L} = 1$. The analysis for $\mathfrak{L} = 0$ can be done in a similar manner. Consequently, we analyze the system in $x \in [A, B]$ and argue that the model can be similarly analyzed in the domain $x \in [C, D]$. Moreover, for simplicity we have assumed the *starting penalty* $R(x_j(t_0)) = R_j(x_0)$ in (21) to be zero. We analyze a few salient characteristics of the socio-technical traffic model: (i) we examine the Fundamental Diagram of the model, (ii) investigate the criteria for hyperbolicity of the model, and (iii) analyze the linear stability based on linearized version of the model, around operating points of the CACC-enabled vehicular traffic.

4.1 Fundamental Diagram

Due to the specific form of functional chosen in (35)-(36), we can calculate the velocity-density relation from (24) to be:

$$u_1 = \mathcal{I} \left(\frac{\partial \mathcal{H}_1}{\partial x}, \rho_1, \alpha \right) = 1 + \frac{\partial \mathcal{H}_1}{\partial x} - \alpha \rho_1, \quad (38)$$

$$u_2 = \mathcal{I} \left(\frac{\partial \mathcal{H}_2}{\partial x}, \rho_2, \alpha \right) = 1 + \frac{\partial \mathcal{H}_2}{\partial x} - (1 - \alpha) \rho_2, \quad (39)$$

Next, let us define the effective densities for the two classes of vehicles $d_1 = \alpha \rho_1$ and $d_2 = (1 - \alpha) \rho_2$. Using (19), the total effective density is given by $d_1 + d_2 = \rho$. Then (38) and (39) can be re-written as

$$u_j = \mathcal{I} \left(\frac{\partial \mathcal{H}_j}{\partial x}, d_j \right) = 1 + \frac{\partial \mathcal{H}_j}{\partial x} - d_j. \quad (40)$$

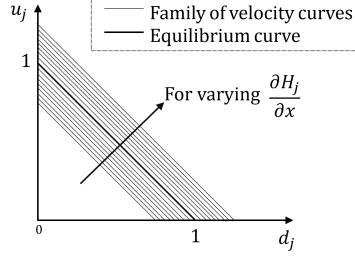


Figure 3: Velocity vs effective density Fundamental Diagram showing variation due to human route choice attribute $\frac{\partial \mathcal{H}_j}{\partial x}$.

This indicates that for the chosen cost functional, velocities of both classes of vehicles depend the optimal driving cost \mathcal{H}_j whereas the latter depends on α (see (21)). This implies that the velocity-effective density relation also implicitly depends on α . Hence, $\frac{\partial \mathcal{H}_j}{\partial x}$ is termed as a human route choice attribute for the Fundamental Diagram.

Now, for equilibrium flow in this linear model, we have $\frac{\partial \mathcal{H}_j}{\partial x} = 0$ [18]. This leads to $u_j = 1 - d_j$ in (40). This implies that under equilibrium condition, both classes of vehicles follow a Greenshields Fundamental Diagram with slope -1 and maximum velocity 1. Now, under non-equilibrium condition, the maximum velocity depends on the socio-technical parameter of each class of vehicles as $u_j|_{max} = 1 + \frac{\partial \mathcal{H}_j}{\partial x}$ while the slope of Fundamental Diagram still being -1 . The effect of the human route choice attribute $\frac{\partial \mathcal{H}_j}{\partial x}$ has been shown in the Fundamental Diagram in Fig. 3.

4.2 Linearized Traffic Model

We can further simplify the system by eliminating \mathcal{H}_j from the equations (38)-(39) using (26)-(27) to obtain:

$$\frac{\partial u_1}{\partial t} + u_1 \frac{\partial u_1}{\partial x} - \alpha \frac{\partial(\rho_1 u_1)}{\partial x} = 0, \quad (41)$$

$$\frac{\partial u_2}{\partial t} + u_2 \frac{\partial u_1}{\partial x} - (1 - \alpha) \frac{\partial(\rho_2 u_2)}{\partial x} = 0. \quad (42)$$

The above equations along with the continuity equations in (25) form the socio-technical model the traffic in this case study. This system of equations can be alternatively written in the form of a conservation law as below:

$$\eta_t + \mathcal{Q}(\eta)_x = 0, \quad (43)$$

where η , defined in (29), denotes the traffic state. The flux \mathcal{Q} of η is given by

$$\mathcal{Q}([\rho_1, u_1, \rho_2, u_2]^T) = \begin{bmatrix} \rho_1 u_1 \\ \frac{u_1^2}{2} - \alpha \rho_1 u_1 \\ \rho_2 u_2 \\ \frac{u_2^2}{2} - (1 - \alpha) \rho_2 u_2 \end{bmatrix}. \quad (44)$$

Since our traffic is assumed to be under CACC control strategy, we can linearize the system around its operating points $\eta^* = [\rho_1^*, u_1^*, \rho_2^*, u_2^*]^T$ for the two classes of vehicles and subsequently analyze its properties from the linearized model. To linearize, we take a Taylor series expansion of \mathcal{Q} around operating point η^* in (43) and neglect higher order terms to obtain:

$$\eta_t + (\partial \mathcal{Q} / \partial \eta)|_{\eta=\eta^*} \eta_x = 0, \quad (45)$$

Here $J = (\partial \mathcal{Q} / \partial \eta)|_{\eta=\eta^*}$ is the Jacobian of the system and is given by

$$J = \frac{\partial \mathcal{Q}}{\partial \eta} \Big|_{\eta=\eta^*} = \begin{bmatrix} A & 0 \\ 0 & B \end{bmatrix}, \quad (46)$$

$$A = \begin{bmatrix} u_1^* & \rho_1^* \\ -\alpha u_1^* & u_1^* - \alpha \rho_1^* \end{bmatrix}, \quad (47)$$

$$B = \begin{bmatrix} u_2^* & \rho_2^* \\ -(1 - \alpha) u_2^* & u_2^* - (1 - \alpha) \rho_2^* \end{bmatrix}. \quad (48)$$

4.3 Hyperbolicity of the Traffic Model

In a qualitative sense, hyperbolicity of a Partial Differential Equation (PDE) system reflects a wave-like nature of its solution. This implies that disturbances to the system propagate at finite speeds along the characteristics of the equations. For a PDE model to be considered as a traffic model, it is imperative to prove that such system is hyperbolic in nature. In this section, we prove that the socio-technical model considered in our case study is strictly hyperbolic.

Definition 1 (Strict hyperbolicity [8]). *A PDE system is strictly hyperbolic if and only if all the eigenvalues of its Jacobian are real and distinct.*

Lemma 1 (Strict hyperbolicity of the socio-technical traffic model). *Consider the multi-class socio-technical traffic model given in (45)-(48). For a given non-zero operating density and velocity for each route $j \in \{1, 2\}$ to be (ρ_j^*, u_j^*) , the traffic model is strictly hyperbolic (with negative definite Jacobian J) if and only if the following conditions are satisfied:*

$$\frac{4u_1^*}{\rho_1^*} < \alpha, \quad \frac{4u_2^*}{\rho_2^*} < (1 - \alpha). \quad (49)$$

Proof. Since $B^2 = 0$, the characteristic equation $\mathcal{P}(\lambda)$ of the Jacobian $\frac{\partial \mathcal{Q}}{\partial \eta}$ simplifies to

$$\mathcal{P}(\lambda) := \det(\lambda I - A) \det(\lambda I - B). \quad (50)$$

The four eigenvalues can be computed from the roots of $\mathcal{P}(\lambda) = 0$ as

$$\lambda_{1,2} = \frac{1}{2} \left[u_1^* - \alpha \rho_1^* \pm \alpha \rho_1^* \sqrt{1 - \frac{4u_1^*}{\alpha \rho_1^*}} \right], \quad (51)$$

$$\lambda_{3,4} = \frac{1}{2} \left[u_2^* - (1 - \alpha) \rho_2^* \pm (1 - \alpha) \rho_2^* \sqrt{1 - \frac{4u_2^*}{(1 - \alpha) \rho_2^*}} \right]. \quad (52)$$

The discriminants here are given by $\Delta_1 = 1 - \frac{4u_1^*}{\alpha \rho_1^*}$, $\Delta_2 = 1 - \frac{4u_2^*}{(1 - \alpha) \rho_2^*}$. It is evident that if the discriminants Δ_1, Δ_2 will be positive, the roots will be real and distinct. Thus under conditions of (49) the eigenvalues of the system are real and distinct and (45) is strictly hyperbolic.

Lastly, since operating density, ρ_j^* , velocity u_j^* and α are all positive, we note here that $\Delta_1, \Delta_2 < 1$. Using (49) with the upper bound on Δ_j , one can easily show that all the eigenvalues $\lambda_m, m \in \{1, 2, 3, 4\}$ are *negative* and J is negative definite. ■

4.4 Linear Stability Analysis

In this subsection, we analyze the linear stability of the traffic model (45).

Definition 2 (Exponential Stability [33]). *The linear hyperbolic system given by (45)-(48) along with its boundary (30) and initial conditions (33) is exponentially stable around operating point η^* in $x \in [A, B]$ if there exists an $\epsilon > 0$ and $0 < M < \infty$ such that for every initial condition $\eta_0 \in L^2([A, B]; \mathbb{R}^4)$, the solution of the boundary value problem satisfies*

$$\|\eta(\cdot, t) - \eta^*\|_{L^2([A, B]; \mathbb{R}^4)} \leq M e^{-\epsilon t} \|\eta_0 - \eta^*\|_{L^2([A, B]; \mathbb{R}^4)}, \quad (53)$$

for all $t \in [0, \infty)$.

Remark 2. *Exponential stability of the traffic system implies that the traffic state η will converge exponentially to operating condition η^* as $t \rightarrow \infty$ given bounded energy error in the initial condition of the system. This indicate that the density and velocity of both the classes of vehicles converge to operating condition as $t \rightarrow \infty$. In other words, $\rho_j \rightarrow \rho_j^*$ and $u_j \rightarrow u_j^*$ for $j \in \{1, 2\}$ as $t \rightarrow \infty$. Additionally, the rate of decay ϵ depends on system characteristics, in particular, on the Jacobian J for our problem. Since, the Jacobian is a function of human route choice attribute α , the convergence also depends on the same.*

Theorem 1 (Exponential Stability Condition). *Consider the Socio-technical hyperbolic traffic model in (45)-(48) along with its boundary (30) and initial conditions (33) that satisfies condition (49). This system is exponentially stable in the sense of (53) around operating point η^* if there exist a $\mu > 0$ such that the matrix \mathcal{J} , given by*

$$\mathcal{J} = J - G_B^T J G_B e^{\mu(A-B)}, \quad (54)$$

is positive definite.

Proof. We define the deviation in the traffic states from the operating point η^* as a new vector

$$E(x, t) = \eta(x, t) - \eta^*. \quad (55)$$

Thereafter, we choose the Lyapunov functional candidate

$$V(t) = \frac{1}{2} \int_A^B e^{-\mu\zeta} E^T(\zeta, t) E(\zeta, t) d\zeta, \quad (56)$$

where $0 < \mu < 1$. We can re-write (56) as

$$V(t) = \frac{1}{2} \|E(\cdot, t) e^{-\frac{\mu}{2}(\cdot)}\|_{L^2([A, B])}^2, \quad (57)$$

where $\|f(\cdot, t)\|_{L^2([A, B])}^2 = \int_A^B f^2(\zeta, t) d\zeta$. The initial condition $V(0)$ is given by $V(0) = \frac{1}{2} \|E(\cdot, 0) e^{-\frac{\mu}{2}(\cdot)}\|_{L^2([A, B])}$.

Taking derivative of $E(t)$ with respect to t yields

$$\begin{aligned} \dot{V}(t) &= \int_A^B e^{-2\mu\zeta} E_t^T(\zeta, t) E(\zeta, t) d\zeta \\ &= e^{-\mu A} E_\zeta^T(A, t) J e(A, t) - e^{-\mu B} E_\zeta^T(B, t) J E(B, t) \\ &\quad + \mu \int_A^B E^T J E e^{-\mu\zeta} d\zeta. \end{aligned} \quad (58)$$

From Lemma 1, we know that the Jacobian J is negative definite which implies there exists $\lambda > 0$ such that $E^T J E \leq -\lambda E^T E$. Additionally, we invoke the boundary condition (30) to obtain

$$\dot{V}(t) \leq -2\mu\lambda V(t) - E^T(A, t) \mathcal{J} E(A, t) e^{-\mu A}, \quad (59)$$

where $\mathcal{J} = J - G_B^T J G_B e^{\mu(A-B)}$. If \mathcal{J} is positive definite, we can write $\dot{V}(t) \leq -2\mu\lambda V(t)$, which implies $V(t) \leq e^{-2\mu\lambda t} V(0)$. Subsequently, we define

$$0 < \gamma_1 = \min_{\zeta \in [A, B]} e^{-\frac{\mu\zeta}{2}} \leq \gamma_2 = \max_{\zeta \in [A, B]} e^{-\frac{\mu\zeta}{2}} < \infty. \quad (60)$$

Using these definitions in (57), initial condition expression $V(0)$, and (60), we can write $\gamma_1^2(B - A) \|E(\cdot, t)\|_{L^2([A, B])}^2 \leq V(t)$ and $V(0) \leq \gamma_2^2(B - A) \|E(\cdot, 0)\|_{L^2([A, B])}^2$. Therefore we obtain

$$\|E(\cdot, t)\|_{L^2([A, B])} \leq \left(\frac{\gamma_2}{\gamma_1}\right) e^{-\mu\lambda t} \|E(\cdot, 0)\|_{L^2([A, B])}. \quad (61)$$

For $0 < M = \frac{\gamma_2}{\gamma_1} < \infty$ and $\epsilon = \mu\lambda > 0$, we proved the socio-technical traffic system (45)-(48) along with its boundary (30) and initial conditions (33) is exponentially stable in the sense of (53). \blacksquare

5 Simulation Results

In this section, we perform simulation studies to illustrate the characteristics of the proposed model, as discussed in previous sections. The distributed plot of the traffic density and velocity for the two classes of the vehicles choosing a route are shown in Fig. 4 and Fig. 5. For this simulation, we have chosen $\alpha = 0.45$. The normalized operating density-velocity pair for the first class has been chosen as (0.85, 0.09,) while for second class it is chosen as (0.75, 0.095). We note here that these operating values satisfy the conditions provided in Lemma 1. The eigenvalues of the Jacobian in this case are $-0.0549, -0.1476, -0.0534$ and -0.1691 . This implies that the simulated socio-technical traffic model is strictly hyperbolic. Moreover, from both Fig. 4 and Fig. 5, we can observe that the system stabilizes to its normalized operating point after perturbation in initial conditions. Hence, the system is stable in the sense of (53).

Next, we investigate the impact of the human route choice attribute α on the socio-technical traffic model. Particularly, we explore the affect of α on the stability of the proposed model. We note that α increases as more and more human passengers choose Route 1. As expected, with increasing α , the density of class 1 vehicles increases and their velocity decreases. This implies that perturbations to the system show larger overshoots in density and takes longer to converge to operating conditions. On the other hand, the contribution of vehicles in class 2 decreases which corresponds to lower density, higher speed and overall faster recovery from perturbations. These phenomena can be observed clearly from Fig. 6, where we plot the spatial norm of the perturbation of traffic density and velocities from operating points of each class. We also note that the simulated system were all stable, as can be seen from the decay of perturbations to zero, albeit at different rates for different α .

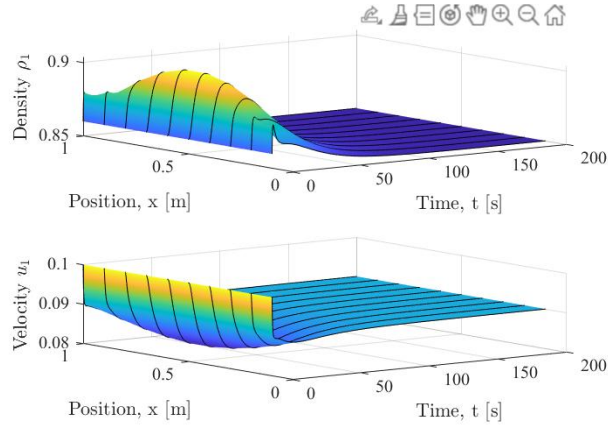


Figure 4: Plot of distributed density and velocity of Class 1 of traffic that chooses Route 1.

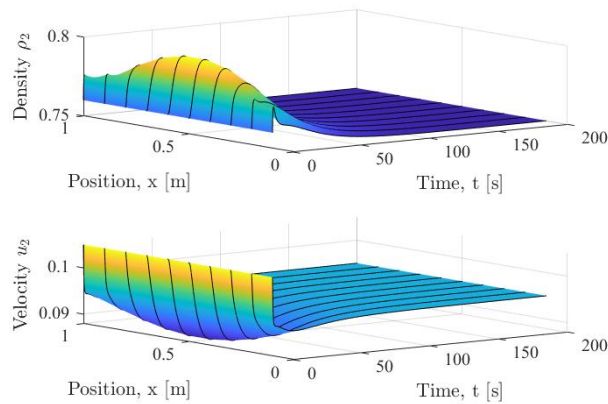


Figure 5: Plot of distributed density and velocity of Class 2 of traffic that chooses Route 2.

6 Conclusion

In this paper, we proposed a socio-technical macroscopic traffic model for CACC enabled vehicles that captures the effect of human passengers' route choice behavior. Essentially, the human passengers' choice of routes leads to multi-class traffic system where each class of vehicles corresponds to each route. First, we have used CPT to model the influence of traffic alerts on human passengers' route choice behavior. Next, we have utilized non-cooperative differential game and MFG to obtain the macroscopic model of a multi-class traffic where the human route choice characterizes the Fundamental Diagram as well as the dynamics of traffic states. To validate the model characteristics, we perform a case study for a particular driving cost function and present simulation results for the same.

References

- [1] AVINERI, E., AND PRASHKER, J. N. Sensitivity to travel time variability: travelers' learning perspective. *Transportation Research Part C: Emerging Technologies* 13, 2 (2005), 157–183.
- [2] BEN-ELIA, E., DI PACE, R., BIFULCO, G. N., AND SHIFTAN, Y. The impact of travel information's accuracy on route-choice. *Transportation Research Part C: Emerging Technologies* 26 (2013), 146–159.
- [3] CARDALIAGUET, P. Notes on mean field games. Tech. rep., Technical report, 2010.
- [4] CHOW, J. Y., LEE, G., AND YANG, I. Genetic algorithm to estimate cumulative prospect theory parameters for selection of high-occupancy-vehicle lane. *Transportation research record* 2157, 1 (2010), 71–77.
- [5] DAVIS, L. Effect of adaptive cruise control systems on traffic flow. *Physical Review E* 69, 6 (2004), 066110.

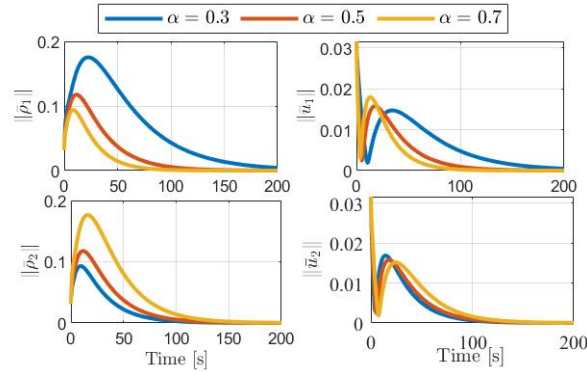


Figure 6: Convergence plots for traffic states' deviations for each class under different values of α .

- [6] DELIS, A. I., NIKOLOS, I. K., AND PAPAGEORGIU, M. Macroscopic traffic flow modeling with adaptive cruise control: Development and numerical solution. *Computers & Mathematics with Applications* 70, 8 (2015), 1921–1947.
- [7] EAGLE, N., AND GREENE, K. *Reality mining: Using big data to engineer a better world*. MIT Press, 2014.
- [8] EVANS, L. *Partial Differential Equations*. Graduate studies in mathematics. American Mathematical Society, 2010.
- [9] FAN, S., AND WORK, D. B. A heterogeneous multiclass traffic flow model with creeping. *SIAM Journal on Applied Mathematics* 75, 2 (2015), 813–835.
- [10] FENNEMA, H., AND WAKKER, P. Original and cumulative prospect theory: A discussion of empirical differences. *Journal of Behavioral Decision Making* 10, 1 (1997), 53–64.
- [11] FOX, C., CAMARA, F., MARKKULA, G., ROMANO, R., MADIGAN, R., MERAT, N., ET AL. When should the chicken cross the road?: Game theory for autonomous vehicle-human interactions.
- [12] GAN, H., AND YE, X. Whether to enter expressway or not? the impact of new variable message sign information. *Journal of Advanced Transportation* 49, 2 (2015), 267–278.
- [13] GAO, S., FREJINGER, E., AND BEN-AKIVA, M. Adaptive route choices in risky traffic networks: A prospect theory approach. *Transportation research part C: emerging technologies* 18, 5 (2010), 727–740.
- [14] GARAVELLO, M., AND PICCOLI, B. *Traffic flow on networks*, vol. 1. American institute of mathematical sciences Springfield, 2006.
- [15] GIGERENZER, G., AND SELTEN, R. *Bounded rationality: The adaptive toolbox*. MIT press, 2002.
- [16] GUAN, Y., ANNASWAMY, A. M., AND TSENG, H. E. Cumulative prospect theory based dynamic pricing for shared mobility on demand services. In *2019 IEEE 58th Conference on Decision and Control (CDC)* (2019), IEEE, pp. 2239–2244.
- [17] HAN, Q., DELLAERT, B. G., VAN RAAIJ, W. F., AND TIMMERMANS, H. J. Integrating prospect theory and stackelberg games to model strategic dyad behavior of information providers and travelers: Theory and numerical simulations. *Transportation research record* 1926, 1 (2005), 181–188.
- [18] HUANG, K., DI, X., DU, Q., AND CHEN, X. Stabilizing traffic via autonomous vehicles: A continuum mean field game approach. In *2019 IEEE Intelligent Transportation Systems Conference (ITSC)* (2019), pp. 3269–3274.
- [19] HUANG, K., DI, X., DU, Q., AND CHEN, X. A game-theoretic framework for autonomous vehicles velocity control: Bridging microscopic differential games and macroscopic mean field games. *Discrete & Continuous Dynamical Systems - B* 25, 12 (2020), 4869–4903.
- [20] JHALA, K., NATARAJAN, B., AND PAHWA, A. Prospect theory-based active consumer behavior under variable electricity pricing. *IEEE Transactions on Smart Grid* 10, 3 (2018), 2809–2819.
- [21] KIRK, D. E. *Optimal control theory: an introduction*. Courier Corporation, 2004.
- [22] LI, N., OYLER, D. W., ZHANG, M., YILDIZ, Y., KOLMANOVSKY, I., AND GIRARD, A. R. Game theoretic modeling of driver and vehicle interactions for verification and validation of autonomous vehicle control systems. *IEEE Transactions on control systems technology* 26, 5 (2017), 1782–1797.

- [23] MILANÉS, V., AND SHLADOVER, S. E. Modeling cooperative and autonomous adaptive cruise control dynamic responses using experimental data. *Transportation Research Part C: Emerging Technologies* 48 (2014), 285–300.
- [24] NGODUY, D. Instability of cooperative adaptive cruise control traffic flow: A macroscopic approach. *Communications in Nonlinear Science and Numerical Simulation* 18, 10 (2013), 2838–2851.
- [25] NIKOLOS, I. K., DELIS, A. I., AND PAPAGEORGIOU, M. Macroscopic modelling and simulation of acc and cacc traffic. In *2015 IEEE 18th International Conference on Intelligent Transportation Systems* (2015), IEEE, pp. 2129–2134.
- [26] NILSSON, H., RIESKAMP, J., AND WAGENMAKERS, E.-J. Hierarchical bayesian parameter estimation for cumulative prospect theory. *Journal of Mathematical Psychology* 55, 1 (2011), 84–93.
- [27] PARZEN, E. On estimation of a probability density function and mode. *The annals of mathematical statistics* 33, 3 (1962), 1065–1076.
- [28] PRELEC, D. The probability weighting function. *Econometrica* 66, 3 (1998), 497–527.
- [29] ROSENBLATT, M. Remarks on some nonparametric estimates of a density function. *Annals of Mathematical Statistics* 27 (1956), 832–837.
- [30] SADIGH, D., SASTRY, S., SESHIA, S. A., AND DRAGAN, A. D. Planning for autonomous cars that leverage effects on human actions. In *Robotics: Science and Systems* (2016), vol. 2, Ann Arbor, MI, USA.
- [31] TALEBPOUR, A., MAHMASSANI, H. S., AND HAMDAR, S. H. Modeling lane-changing behavior in a connected environment: A game theory approach. *Transportation Research Part C: Emerging Technologies* 59 (2015), 216–232.
- [32] TVERSKY, A., AND KAHNEMAN, D. Advances in prospect theory: Cumulative representation of uncertainty. *Journal of Risk and uncertainty* 5, 4 (1992), 297–323.
- [33] VAMVOUDAKIS, K., AND JAGANNATHAN, S. *Control of Complex Systems: Theory and Applications*. Butterworth-Heinemann, 2016.
- [34] WANG, M., DAAMEN, W., HOOGENDOORN, S. P., AND VAN AREM, B. Rolling horizon control framework for driver assistance systems. part i: Mathematical formulation and non-cooperative systems. *Transportation research part C: emerging technologies* 40 (2014), 271–289.
- [35] WANG, M., DAAMEN, W., HOOGENDOORN, S. P., AND VAN AREM, B. Rolling horizon control framework for driver assistance systems. part ii: Cooperative sensing and cooperative control. *Transportation research part C: emerging technologies* 40 (2014), 290–311.
- [36] WANG, M., TREIBER, M., DAAMEN, W., HOOGENDOORN, S. P., AND VAN AREM, B. Modelling supported driving as an optimal control cycle: Framework and model characteristics. *Transportation Research Part C: Emerging Technologies* 36 (2013), 547–563.
- [37] WANG, S., AND ZHAO, J. How risk preferences influence the usage of autonomous vehicles. Tech. rep., 2018.
- [38] WHITWORTH, B., AND AHMAD, A. *The social design of technical systems: Building technologies for communities*. Interaction Design Foundation, 2013.
- [39] WONG, T. W., SAXENA, N., AND DIXIT, V. V. A study of route choice behavior of drivers in autonomous vehicles. Tech. rep., 2018.
- [40] WU, Y., XU, C., AND ZHANG, T. Evaluation of renewable power sources using a fuzzy mcdm based on cumulative prospect theory: A case in china. *Energy* 147 (2018), 1227–1239.
- [41] XIAO, L., WANG, M., AND VAN AREM, B. Realistic car-following models for microscopic simulation of adaptive and cooperative adaptive cruise control vehicles. *Transportation Research Record* 2623, 1 (2017), 1–9.
- [42] XU, D., XIAO, L., MANDAYAM, N. B., AND POOR, H. V. Cumulative prospect theoretic study of a cloud storage defense game against advanced persistent threats. In *2017 IEEE Conference on Computer Communications Workshops (INFOCOM WKSHPS)* (2017), IEEE, pp. 541–546.
- [43] XU, H., ZHOU, J., AND XU, W. A decision-making rule for modeling travelers’ route choice behavior based on cumulative prospect theory. *Transportation Research Part C: Emerging Technologies* 19, 2 (2011), 218–228.
- [44] YU, H., TSENG, H. E., AND LANGARI, R. A human-like game theory-based controller for automatic lane changing. *Transportation Research Part C: Emerging Technologies* 88 (2018), 140–158.
- [45] ZHANG, C., LIU, T.-L., HUANG, H.-J., AND CHEN, J. A cumulative prospect theory approach to commuters’ day-to-day route-choice modeling with friends’ travel information. *Transportation Research Part C: Emerging Technologies* 86 (2018), 527–548.